Canonical and grand canonical ensemble expectation values from quantum Monte Carlo simulations

R. D. Sedgewick, D. J. Scalapino, and R. L. Sugar
Department of Physics, University of California, Santa Barbara, California 93106, USA

L. Capriotti
Kavli Institute for Theoretical Physics, University of California, Santa Barbara, California 93106, USA

(Received 14 February 2003; published 30 July 2003)

We present a method for obtaining grand canonical expectation values as a continuous function of the chemical potential in quantum Monte Carlo simulations. We show how canonical ensemble expectation values can be extracted in such simulations. In order to obtain results for all particle sectors, a modest number of grand canonical simulations must be performed, each at a different chemical potential. With the canonical ensemble results in hand, grand canonical expectation values can be constructed for arbitrary dopings. Results are presented from the application of this method to the two-dimensional Hubbard model.

DOI: 10.1103/PhysRevB.68.045120 PACS number(s): 71.10.Fd, 71.15.Dx, 05.10.Ln

I. INTRODUCTION

The properties of strongly correlated electron systems near the Mott insulating phase depend sensitively on the doping.[1] Most simulations of these systems have been carried out within the grand canonical ensemble, where a convenient formalism exists for the evaluation of finite-temperature Green's functions and other physical quantities that can be expressed in terms of them.[2] In this framework, to explore the doping dependence, it is necessary to carry out simulations at various discrete values of the chemical potential $\{\mu_\alpha\}$ and interpolate between them. In this paper we describe a method for optimally combining data from these simulations to obtain results for a continuous range of μ. We first evaluate canonical ensemble expectation values and partition functions (up to an overall constant) from simulations performed in the grand canonical ensemble. Using the approach of Ferrenberg and Swendsen[3] to combine results from simulations performed with different values of the chemical potential, we obtain canonical ensemble quantities for a wide range of fillings from a modest number of simulations. From these we are able to construct grand canonical expectation values, enabling us to study a variety of physical quantities as a continuous function of the chemical potential.

In Sec. II we present our methodology, and in Sec. III we illustrate it with results for the two-dimensional Hubbard model.

II. METHODOLOGY

We begin by briefly summarizing the approach to the simulation of strongly correlated many-electron systems in the grand canonical ensemble set out in Ref. 2. The expectation value of a physical observable O is

$$\langle O(\mu)\rangle = \frac{\mathrm{Tr}[Oe^{-\beta(H-\mu N)}]}{\mathrm{Tr}[e^{-\beta(H-\mu N)}]}, \tag{1}$$

where H is the Hamiltonian, β the inverse temperature, μ the chemical potential, and N the number operator for the electrons. In order to perform a numerical simulation, one must first evaluate the traces over the electron degrees of freedom. This is possible if the Hamiltonian is quadratic in the electron creation and annihilation operators or can be made so through a Hubbard-Stratonovich transformation. To this end we introduce a small imaginary-time step $\Delta\tau$ by writing $\beta = \Delta\tau L$. The partition function can then be written in the form

$$Z(\mu) = \mathrm{Tr}[e^{-\beta(H-\mu N)}] = \mathrm{Tr}[e^{-\Delta\tau(H-\mu N)}]^L. \tag{2}$$

For each time slice $\ell = 1, \ldots, L$, we introduce a set of Hubbard-Stratonovich variables $x(\ell)$ such that

$$e^{-\Delta\tau H} = \sum_{x(\ell)} \omega(x(\ell)) \exp\left(-\Delta\tau \sum_{i,j,\sigma} c^\dagger_{i\sigma} h^\sigma_{i,j}(x(\ell)) c_{j\sigma} \right). \tag{3}$$

Here $c^\dagger_{i\sigma}$ and $c_{i\sigma}$ are the creation and annihilation operators for electrons at lattice site i with z component of spin σ, $h^\sigma_{i,j}(x(\ell))$ is a single-particle Hamiltonian for an electron propagating through the external field $x(\ell)$, and $\omega(x(\ell))$ is a positive-definite weight function. $\Sigma_{x(\ell)}$ indicates a sum over discrete Hubbard-Stratonovich variables. Here and in succeeding formulas, the sums would be replaced by integrals for continuous Hubbard-Stratonovich variables. Typically, x_ℓ has a component for each spatial lattice site or link.

The traces in Eq. (1) can now be performed, yielding an expression of the general form

$$\langle O(\mu)\rangle = \frac{\sum_x \rho(x,\mu) O(x,\mu)}{\sum_{x'} \rho(x',\mu)}. \tag{4}$$

Here x stands for the totality of Hubbard-Stratonovich variables on all time slices,

$$\rho(x,\mu) = D_\uparrow(x,\mu) D_\downarrow(x,\mu) \prod_{\ell=1}^{L} \omega(x(\ell)), \tag{5}$$

and the determinants for spin-up and -down electrons are given by

$$D_\sigma(x,\mu) = \mathrm{Det}[I + e^{\beta\mu} A_\sigma(x)], \tag{6}$$

where I is the unit matrix and

$$A_\sigma(x) = e^{-\Delta\tau h^\sigma(x(L))} \cdots e^{-\Delta\tau h^\sigma(x(1))}. \tag{7}$$

The quantity $O(x,\mu)$ in Eq. (4) can generally be expressed in terms of finite-temperature Green's functions for a single electron propagating in the background field provided by the Hubbard-Stratonovich variables x. For example,

$$\mathrm{Tr}[c_{i\sigma} c^\dagger_{j\sigma'} e^{-\beta(H-\mu N)}]$$

$$= D_\uparrow(x,\mu) D_\downarrow(x,\mu) \delta_{\sigma,\sigma'} \left(\frac{1}{I + e^{\beta\mu} A_\sigma(x)} \right)_{i,j}.$$

For models with particle-hole symmetry, such as the Hubbard model at half-filling, the product of the electron determinants is positive, and one can use importance sampling techniques to generate a sequence of Hubbard-Stratonovich configurations with the probability distribution

$$P(x,\mu) = \frac{\rho(x,\mu)}{\sum_{x'} \rho(x',\mu)}. \tag{8}$$

The average value of $O(x,\mu)$ in these configurations is then an estimator for $\langle O(\mu) \rangle$. Details of an algorithm for efficiently generating configurations are given in Ref. 2.

For systems which do not have particle-hole symmetry, such as the Hubbard model away from half-filling, the product of electron determinants will in general not be positive definite. In such cases, one can generate Hubbard-Stratonovich fields using the probability distribution

$$P_{||}(x,\mu) = \frac{|\rho(x,\mu)|}{\sum_{x'} |\rho(x',\mu)|}. \tag{9}$$

It is then necessary to move the sign of $\rho(x,\mu)$,

$$S(x,\mu) = \frac{\rho(x,\mu)}{|\rho(x,\mu)|} = \pm 1, \tag{10}$$

into the measurements yielding

$$\langle O(\mu) \rangle = \sum_x P(x,\mu) O(x,\mu)$$

$$= \frac{\sum_x P_{||}(x,\mu) O(x,\mu) S(x,\mu)}{\sum_{x'} P_{||}(x',\mu) S(x',\mu)}. \tag{11}$$

The expectation value of the sign can be written

$$\langle S(\mu) \rangle = \sum_x P_{||}(x,\mu) S(x,\mu) = \frac{\sum_x \rho(x,\mu)}{\sum_{x'} |\rho(x',\mu)|} = \frac{Z(\mu)}{Z_{||}(\mu)}. \tag{12}$$

Here $Z(\mu)$ is the partition function of the physical system and $Z_{||}(\mu)$ that of a fictitious one in which the sign of the product of determinants, $S(x,\mu)$, is ignored.

To obtain information about the canonical ensemble from grand canonical simulations, we note that as long as the electron number operator commutes with the Hamiltonian and the Hubbard-Stratonovich variables are chosen so that Eq. (3) holds, then the product of electron determinants has an expansion in the fugacity of the form

$$D_\uparrow(x,\mu) D_\downarrow(x,\mu) = \sum_N Z_N(x) e^{\beta\mu N}. \tag{13}$$

Once we have gone to the computational expense of performing a matrix decomposition of $A_\sigma(x)$, Eq. (7), which we must do each time we make a measurement,[2] it is straightforward to evaluate the left-hand side of Eq. (13) for a number of different values of μ. Equation (13) then yields a set of linear equations that can be solved for the $Z_N(x)$. At moderate to low temperatures, only a limited subset of the $Z_N(x)$ will make a significant contribution to the product of determinants, so the system of equations to be solved is considerably smaller than the number of spatial lattice points. Since the canonical partition function for the sector with electron number N is given by

$$\sum_x \frac{P_{||}(x,\mu) Z_N(x)}{|D_\uparrow(x,\mu) D_\downarrow(x,\mu)|} = \frac{Z_N}{Z_{||}(\mu)} \equiv \tilde{Z}_N(\mu), \tag{14}$$

where

$$Z_N = \sum_x Z_N(x) \prod_{\ell=1}^{L} \omega(x(\ell)), \tag{15}$$

we can evaluate $\tilde{Z}_N$ using an ensemble of Hubbard-Stratonovich fields generated with the probability distribution $P_{||}(x,\mu)$.

If the operator O is defined on a single imaginary-time slice or if it does not change the electron number from time slice to time slice, then we can also write

$$O(x,\mu) D_\uparrow(x,\mu) D_\downarrow(x,\mu) = \sum_N O_N(x) e^{\beta\mu N}, \tag{16}$$

and we can obtain a set of linear equations for the $O_N(x)$ by evaluating the left-hand side of Eq. (16) for different values of μ. In this case,

$$\sum_x \frac{P_{||}(x,\mu) O_N(x)}{|D_\uparrow(x,\mu) D_\downarrow(x,\mu)|} = \frac{O_N}{Z_{||}(\mu)} \equiv \tilde{O}_N(\mu). \tag{17}$$

Finally, the expectation value of the operator O in the canonical ensemble sector with electron number N is

$$\langle O\rangle_N=\frac{\tilde{O}_N}{\tilde{Z}_N}=\frac{O_N}{Z_N}. \tag{18}$$

Also, once the Z_N and O_N are in hand,

$$\langle O\rangle=\frac{\sum_N O_N e^{\beta\mu N}}{\sum_N Z_N e^{\beta\mu N}} \tag{19}$$

gives the grand canonical expectation values as continuous functions of μ.

From simulations at a single value of μ one only expects to be able to make accurate determinations of the Z_N and O_N for N in the vicinity of $\langle N\rangle$. We must therefore perform a set of simulations with chemical potentials μ_α, sufficiently spaced to cover the range of N relevant to the problem of interest. As indicated in Eqs. (14) and (17), the outputs of our simulations are $\tilde{Z}_N(\mu_\alpha)=Z_N/Z_{||}(\mu_\alpha)$ and $\tilde{O}_N(\mu_\alpha)=O_N/Z_{||}(\mu_\alpha)$, rather than Z_N and O_N. We can combine results from simulations with different values of the chemical potential by writing

$$Z_N=\sum_\alpha c_\alpha \tilde{Z}_N(\mu_\alpha) Z_{||}(\mu_\alpha), \tag{20}$$

$$O_N=\sum_\alpha d_\alpha \tilde{O}_N(\mu_\alpha) Z_{||}(\mu_\alpha), \tag{21}$$

with

$$\sum_\alpha c_\alpha=\sum_\alpha d_\alpha=1. \tag{22}$$

Following Ferrenberg and Swendsen, we choose the c_α and d_α to minimize the variance of Z_N and O_N subject to the constraints of Eq. (22). A short calculation yields

$$c_\alpha=\frac{1/[Z_{||}(\mu_\alpha)\sigma_N^2(\mu_\alpha)]}{\sum_\gamma 1/[Z_{||}(\mu_\gamma)\sigma_N^2(\mu_\gamma)]}, \tag{23}$$

where $\sigma_N^2(\mu_\alpha)$ is the variance of $\tilde{Z}_N(\mu_\alpha)$, which we determine from the simulation. Of course, a corresponding result holds for the d_α with $\sigma_N^2(\mu_\alpha)$ replaced by the variance of the $\tilde{O}_N(\mu_\alpha)$.

The constants $Z_{||}(\mu_\alpha)$ can be determined up to an overall normalization by iteratively solving the equation

$$Z(\mu_\alpha)=Z_{||}(\mu_\alpha)\langle S(\mu_\alpha)\rangle=\sum_N Z_N e^{\beta\mu_\alpha N}, \tag{24}$$

with the Z_N given by Eqs. (20) and (23). The $\langle S(\mu_\alpha)\rangle$ are measured directly in the simulations.

It is also possible to obtain $Z_{||}(\mu)$, and therefore $\langle S(\mu)\rangle$, as a continuous function of μ. We simply note that

$$Z_{||}(\mu)=\sum_N Z_{N||}(\mu) e^{\beta\mu N}, \tag{25}$$

where

$$Z_{N||}(\mu)=\sum_x Z_N(x) S(x,\mu) \prod_{\ell=1}^{L} \omega(x(\ell)). \tag{26}$$

Note that once the $Z_N(x)$ are known for any configuration, we can determine $S(x,\mu)$ for any value of μ from the right-hand side of Eq. (13). A simulation performed at the chemical potential μ_α will, of course, only determine the ratio $Z_{N||}(\mu)/Z_{||}(\mu_\alpha)$. However, we can combine results from simulations performed at different values of the chemical potential just as for the Z_N.

III. NUMERICAL RESULTS

We illustrate the methodology outlined in the last section with results for the two-dimensional Hubbard model. The Hamiltonian is

$$H=-t\sum_{\langle ij\rangle,\sigma}(c_{i\sigma}^\dagger c_{j\sigma}+c_{j\sigma}^\dagger c_{i\sigma})+U\sum_i\left(n_{i\uparrow}-\frac{1}{2}\right)\left(n_{i\downarrow}-\frac{1}{2}\right). \tag{27}$$

Here $c_{i\sigma}^\dagger$ and $c_{i\sigma}$ are the creation and annihilation operators for electrons with z component of spin σ at lattice site i, and $n_{i\sigma}=c_{i\sigma}^\dagger c_{i\sigma}$. The sum $\langle ij\rangle$ is over all pairs of nearest-neighbor lattice sites. t is the hopping parameter and U the Coulomb coupling constant.

The Coulomb term is reduced to quadratic form in the electron creation and annihilation operators using Hirsch's discrete Hubbard-Stratonovich transformation[4]

$$e^{-\Delta\tau U(n_{i\uparrow}-1/2)(n_{i\downarrow}-1/2)} = \frac{1}{2}e^{-\Delta\tau U/4}\sum_{x_i(\ell)=\pm1} e^{-\Delta\tau x_i(\ell)\lambda(n_{i\uparrow}-n_{i\downarrow})}. \tag{28}$$

For $\mu=0$, which corresponds to half-filling, particle-hole symmetry implies that $D_\uparrow(x,0)D_\downarrow(x,0)$ is always positive,[4] so $S(x,0)=1$, and there is no sign problem. It is therefore convenient to adopt the normalization $Z_{||}(0)=Z(0)=1$ in solving Eq. (24) for $Z_{||}(\mu_\alpha)$. Thus, we are in fact able to use Eqs. (24) and (25) to determine $Z(\mu)/Z(0)$ and $Z_{||}(\mu)/Z_{||}(0)$, respectively.

All of the results we present here are on a 4×4 lattice with $t=1$ and $U=4$. The number of time slices, L, is chosen so that $\Delta\tau=1/8$. Except where otherwise noted, simulations were performed at $\mu=-1.5$, $\mu=-1.025$, and $\mu=-0.6$ for each temperature. At $\beta=8$ we performed additional runs at both $\mu=-0.9625$ and $\mu=-0.9$, while at other temperatures either $\mu=-0.9625$ or $\mu=-0.90$ was used. For runs at $\mu=-0.6$, 100 000 Monte Carlo sweeps with 10 000 warmup sweeps were performed. For all other runs, 400 000 Monte Carlo sweeps with 10 000 warmup sweeps were performed. For all simulations, nonlocal moves, as suggested in Ref. 5,

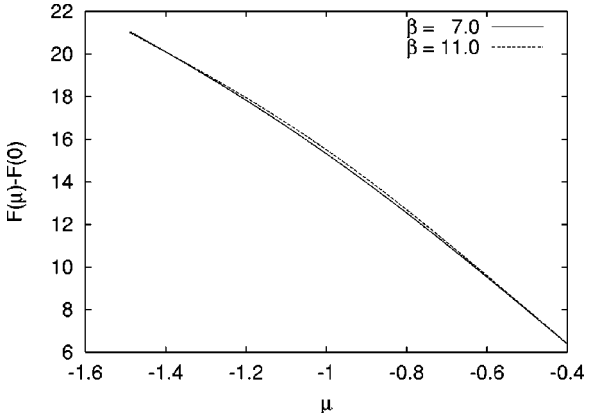

FIG. 1. Free energy difference between half-filled system and system with chemical potential μ. Statistical errors are negligible on this scale.

were used to assure ergodicity. To invert Eqs. (13) and (16), the right-hand sides are measured at the set of chemical potentials,

$$\mu(i)=\mu_\alpha+i\,\delta\mu, \tag{29}$$

where μ_α is the chemical potential used in the simulation, $i=-7,\ldots,0,\ldots,7$ and $\delta\mu=0.02$. After inversion and averaging over configurations, particle sectors where $Z_N e^{\beta\mu_\alpha N}/Z(\mu_\alpha)<10^{-4}$ are dropped to prevent the spread of roundoff error from the inversion. The jackknife method was used for error analysis. It should be noted that, after analysis, results at different values of μ are not statistically independent.

In Fig. 1 we plot the free energy difference

$$F(\mu)-F(0)=-\frac{1}{\beta}\ln\{Z(\mu)/Z(0)\} \tag{30}$$

as a function of μ for two values of β. In Fig. 2 we plot the density defined by $n(\mu)=\langle N\rangle/V$. Here V is the number of spatial lattice points and $\langle N\rangle$ is calculated using the standard thermodynamic identity,

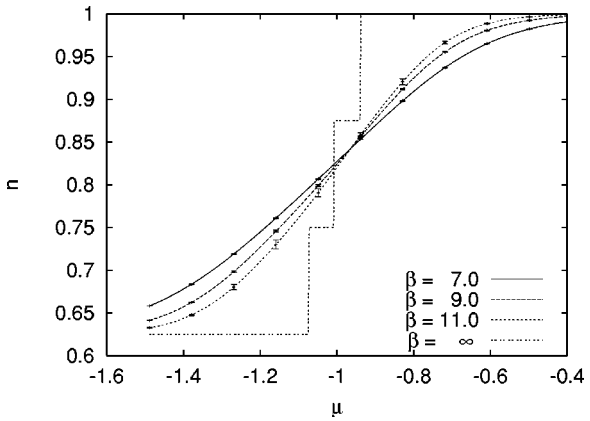

FIG. 2. Density of the system for several different values of β. As errors depend on μ, error bars are shown at several points along the curves here and in subsequent figures. Also shown is the zero-temperature result, calculated using exact diagonalization.

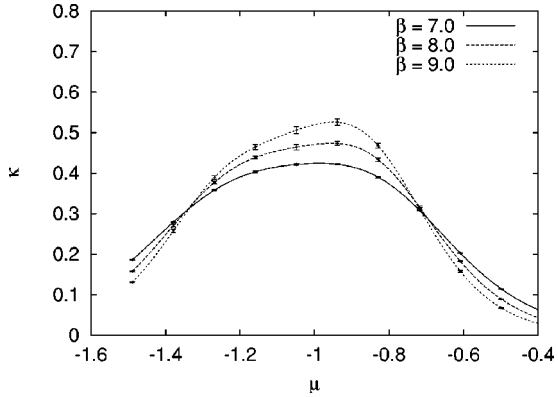

FIG. 3. Charge compressibility of the system, obtained by the analytical differentiation of n.

$$\langle N\rangle=-\frac{\partial F}{\partial\mu}=\frac{\sum_N NZ_N e^{\beta\mu N}}{\sum_N Z_N e^{\beta\mu N}}. \tag{31}$$

As the temperature is lowered, the transition between the half-filled state ($n=1.0$) and the six-hole state ($n=0.625$) becomes sharper. In particular, at zero temperature the density decreases in a series of jumps, due to the discreteness of the finite-size spectrum.

Within our framework it is also straightforward to compute the compressibility of the system, $\kappa=\partial n/\partial\mu$, by differentiation of Eq. (31). Note that the differentiation can be performed analytically. Figure 3 shows the compressibility as a function of μ for different values of β. As the temperature is lowered, the compressibility develops a peak around $\mu=-1.0$ that is likely to be the signature of the low-temperature divergence expected from the metal-insulator transition.[6]

As previously mentioned, within our numerical scheme it is possible to calculate observables that are not diagonal in the particle number. Figure 4(a) shows the antiferromagnetic structure factor. This is given by

$$S^{zz}(\pi,\pi)=\frac{1}{V}\sum_{ij}(-1)^{i+j}S_i^z S_j^z, \tag{32}$$

where $S_i^z=\frac{1}{2}c_{i\alpha}^\dagger\sigma_{\alpha\beta}^z c_{i\beta}$ is the standard spin operator. The plot of this quantity versus μ clearly indicates that the antiferromagnetic correlations present at half-filling are sharply suppressed upon doping. A similar plot of the equal-time d-wave pair field correlation function is shown in Fig. 4(b). Here the d-wave pair field correlation function is given by

$$\rho_d=\frac{1}{V}\sum_{ij}\Delta_i\Delta_j^\dagger, \tag{33}$$

where $\Delta_i^\dagger=\frac{1}{2}\Sigma_\delta(-1)^\delta c_{i\uparrow}^\dagger c_{i+\delta\downarrow}^\dagger$ creates two electrons in a d state. Here, δ sums over the four near-neighbor sites of l and $(-1)^\delta$ gives the sign alternation characteristic of a d-wave pairing amplitude. The enhancement of ρ_d toward $\mu=0.0$ is

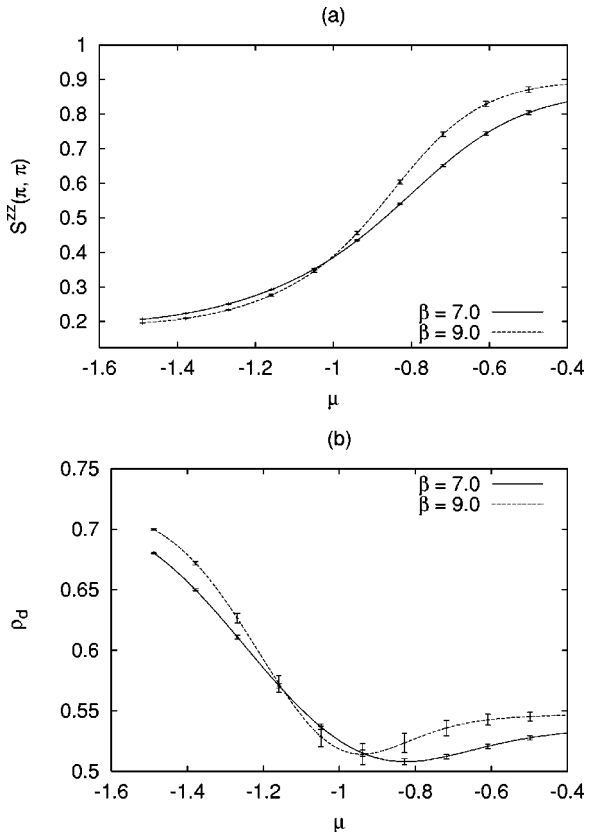

FIG. 4. (a) The antiferromagnetic structure factor $S^{zz}(\pi,\pi)$. (b) The *d*-wave pair field correlation function.

a finite-size effect due to a strong antiferromagnetic response in the nearest-neighbor terms in Eq. (33).

Finally, we show the expectation value of the sign in Fig. 5. Here the sign is calculated as a continuous function of μ using Eqs. (25) and (26). Note that the sign is small in the $\mu=-1.0$ region where the density is changing rapidly and electron correlations are believed to be important. In this region the variance of the sign decreases as the sign does, but the fractional error increases, becoming as large as 2% for $\beta=8$ and 12% for $\beta=10$. Naturally, the variance of physical observables grows as the fractional error of the sign does.

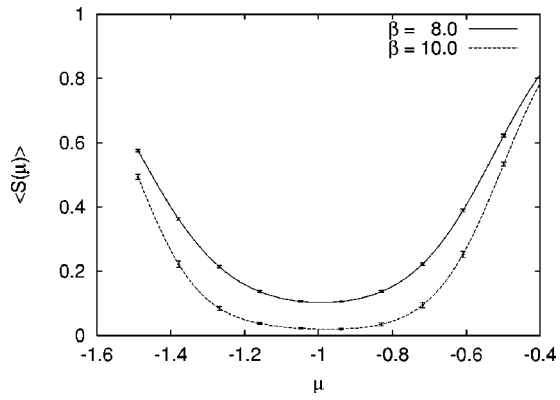

FIG. 5. The expectation value of the sign. Calculated from runs with 100 000 Monte Carlo sweeps at $\mu=-1.5$, $\mu=-1.025$, and $\mu=-0.6$.

IV. CONCLUSION

In this paper we have presented a method for extracting canonical ensemble results from grand canonical ensemble quantum Monte Carlo simulations. As canonical information is only extracted from sectors whose particle number is close to the average number of particles in the simulation, simulations must be performed at several different chemical potentials to obtain results for a range of particle number sectors. These separate simulations can then be combined to obtain a complete picture of the different canonical ensembles with lower statistical fluctuations than any of the simulations taken individually. Once the canonical results are obtained, they can be combined to give grand canonical results as a continuous function of the chemical potential.

In this work we have presented results for the two-dimensional Hubbard model on a 4×4 lattice with Coloumb interactions of moderate strength, but the method is applicable to any quantum mechanical problem, simulated in the grand canonical ensemble, for which particle number is conserved.

ACKNOWLEDGMENTS

We would like to thank R.T. Scalettar and A. Sandvik for insightful discussions and Federico Becca for help with the Lanczos calculations. This work was supported by the Department of Energy under Grant No. DOE85-45197.

[1] E.W. Carlson, V.J. Emergy, S.A. Kivelson, and D. Orgad, cond-mat/0206217; in *The Physics of Semiconductors*, Vol. 1: *Conventional and High-T_c Superconductors*, edited by K.H. Bennemann and J.B. Ketterson (Springer-Verlag, New York, 2003).

[2] R. Blankenbecler, D.J. Scalapino, and R.L. Sugar, Phys. Rev. D **24**, 2278 (1981); S.R. White, D.J. Scalapino, R.L. Sugar, E.Y. Loh, J.E. Gubernatis, and R.T. Scalettar, Phys. Rev. B **40**, 506 (1989).

[3] A.M. Ferrenberg and R.H. Swendsen, Phys. Rev. Lett. **63**, 1195 (1989).

[4] J.E. Hirsch, Phys. Rev. B **31**, 4403 (1985).

[5] R.T. Scalettar, R.M. Noack, and R.R.P. Singh, Phys. Rev. B **44**, 10 502 (1991).

[6] N. Furukawa and M. Imada, J. Phys. Soc. Jpn. **60**, 3604 (1991).